Electronic supporting information for：

Ionothermal confined self-organization for hierarchical porous magnesium borate superstructures and their application as adsorbents for efficient dye removal

Zhaoqiang Zhang[a], Wancheng Zhu[a,], Ruguo Wang[a], Linlin Zhang[a], Lin Zhu[a], Qiang Zhang[b,*]*

[a] Department of Chemical Engineering, Qufu Normal University, Shandong 273165, China.

[b] Beijing Key Laboratory of Green Chemical Reaction Engineering and Technology, Department of Chemical Engineering, Tsinghua University, Beijing 100084, China.

---

[*] Corresponding author. Tel.: +86-537-4453130; fax: +86-10-62772051.

E-mail: zhuwancheng@tsinghua.org.cn (W. Zhu); zhang-qiang@mails.tsinghua.edu.cn (Q. Zhang).

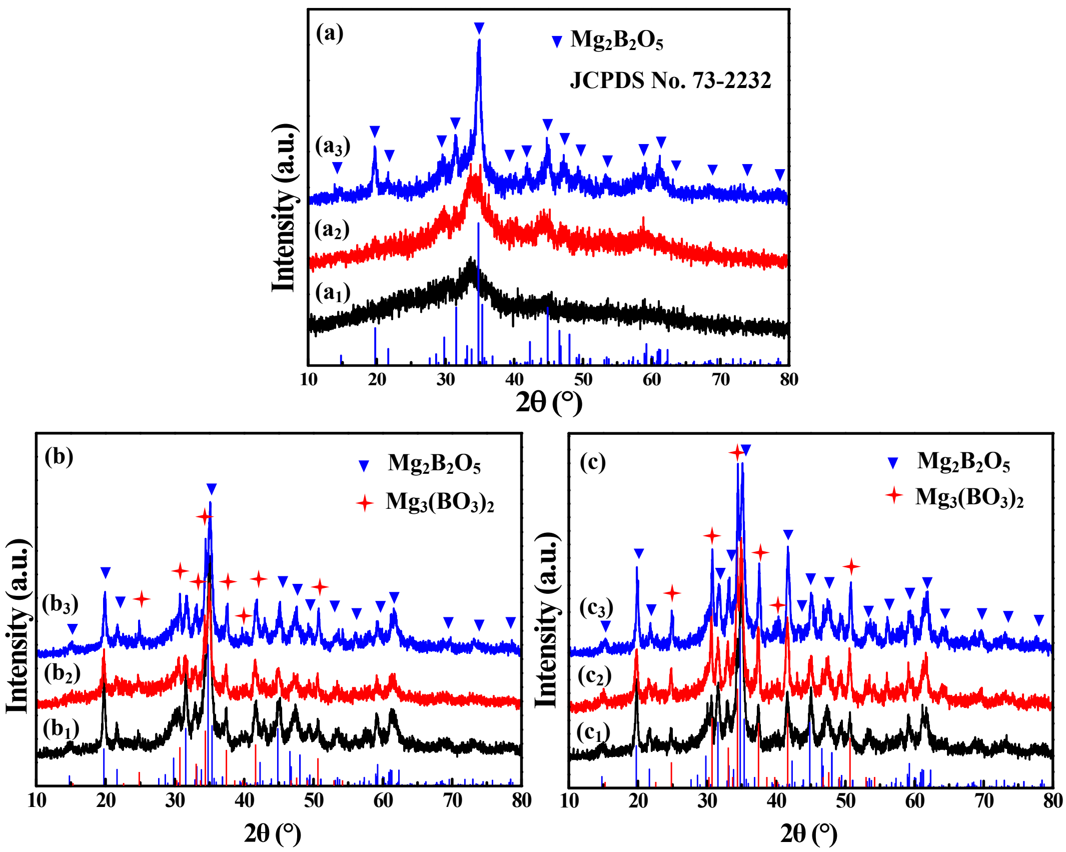

Fig. S1. $MgBO_2(OH)$ calcined with various heating procedures. Temperature (ºC): (a)-600, (b)-650, (c)-700; time (h): (a_1,b_1,c_1)-2.0, (a_2,b_2,c_2)-4.0, (a_3,b_3,c_3)-8.0; heating-rate (ºC min^{-1}): (a_1,b_1,c_1)-2, (a_2,b_2,c_2)-5, (a_3,b_3,c_3)-10. Vertical lines: red-standard pattern of $Mg_3(BO_3)_2$ (JCPDS No. 33-0858), blue-standard pattern of triclinic $Mg_2B_2O_5$ (JCPDS No. 73-2232).

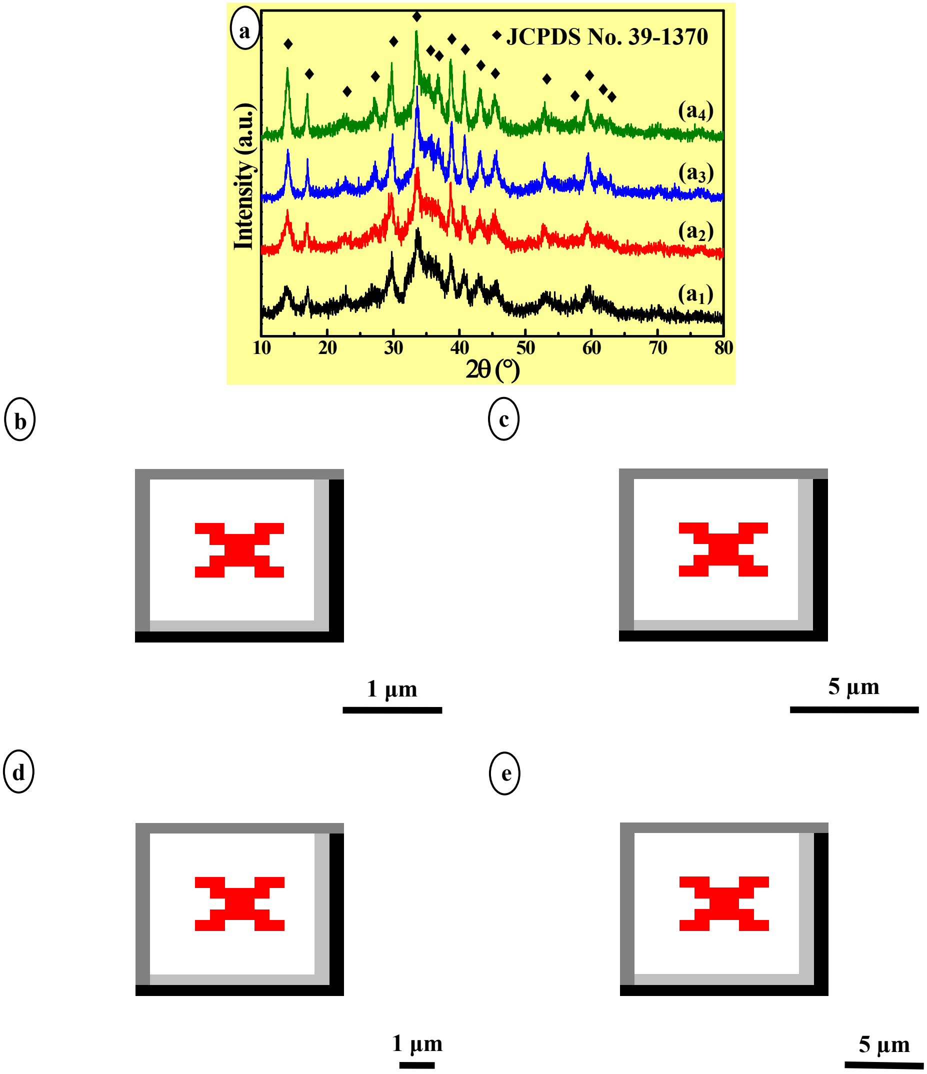

Fig. S2. XRD patterns (a) and morphology evolution (b-e) of the ionothermal products formed at various temperatures for 12.0 h. Temperature (ºC): (a_1, b)-120, (a_2, c)-140, (a_3, d)-160, (a_4, e)-180.

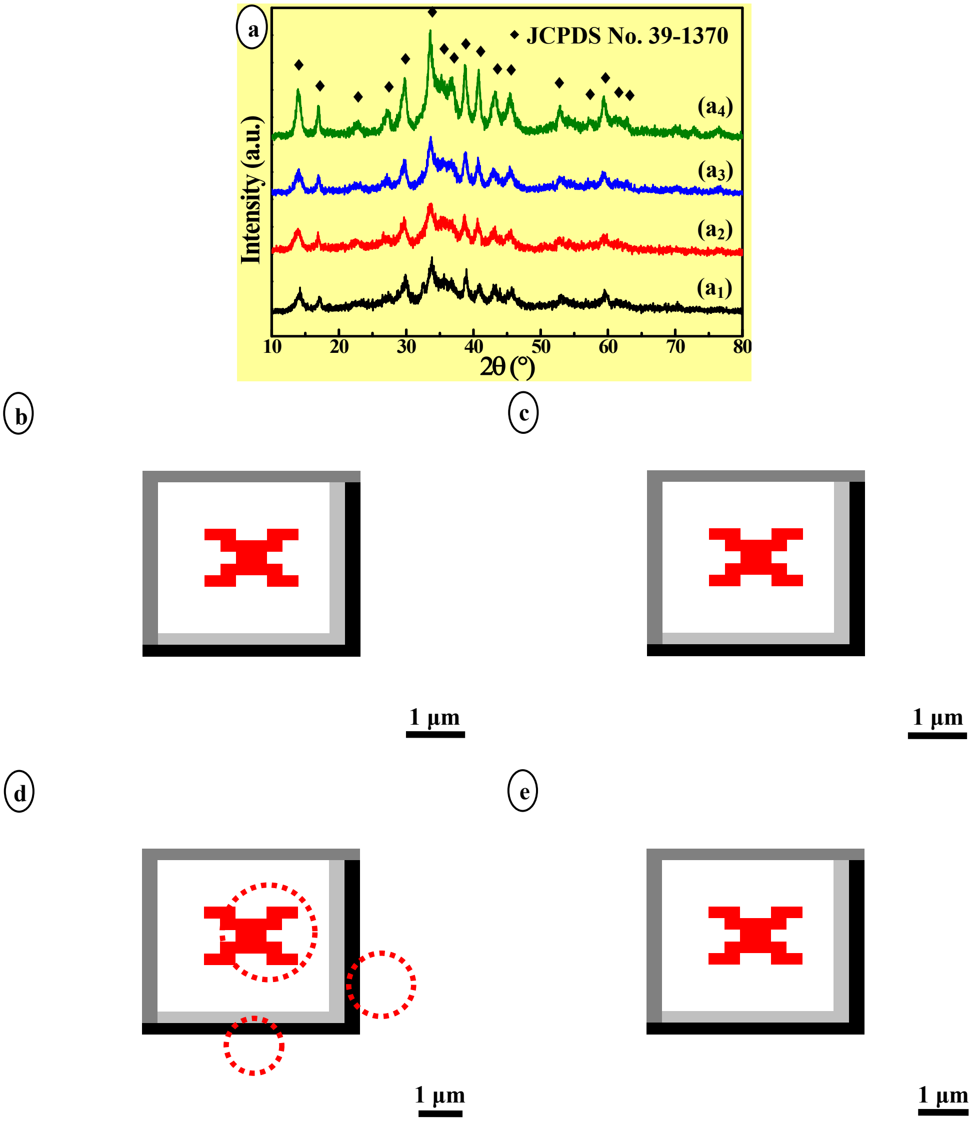

Fig. S3. XRD patterns (a) and morphology evolution (b-e) of the ionothermal products obtained at 150 ºC at different growth durations. Time (h): (a_1, b)-6.0, (a_2, c)-8.0, (a_3, d)-10.0, (a_4, e)-16.0.

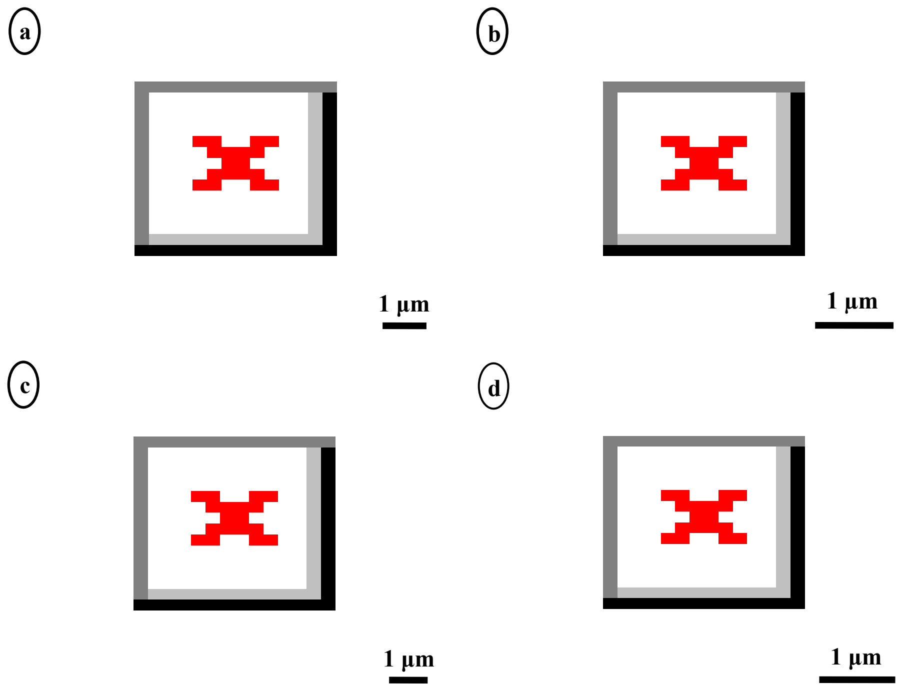

Fig. S4. Morphology evolution of the $MgBO_2(OH)$ nanostructures obtained at 150 ºC for 12.0 h by using different volume ratios of ILs / water as media. Volume ratio of ILs / water: (a)-8/1, (b)-3/1, (c)-2/1, (d)-0/1.

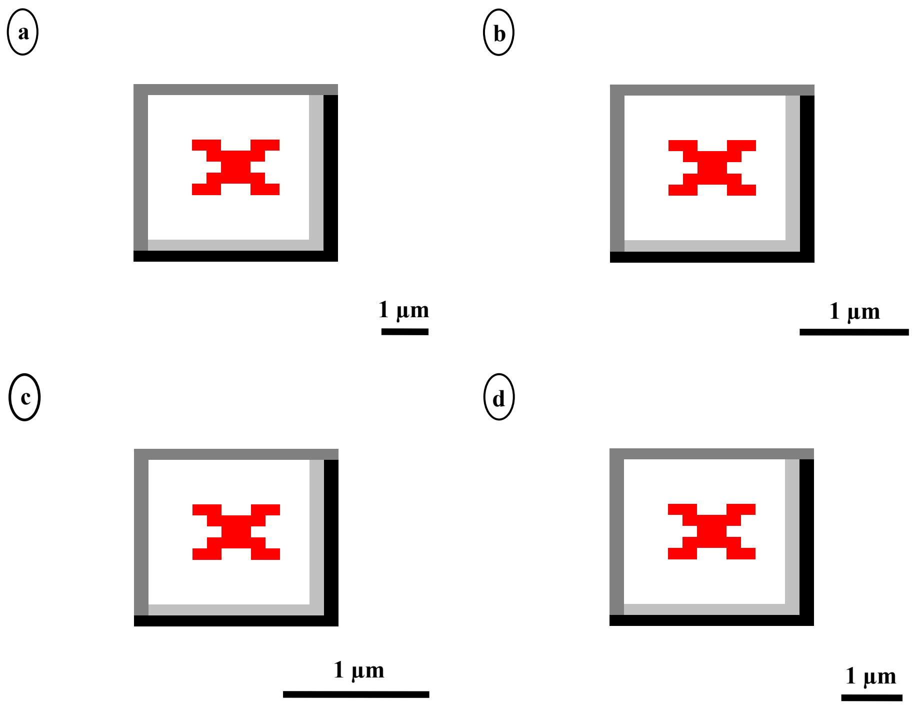

Fig. S5. $MgBO_2(OH)$ obtained at 150 ºC for 12.0 h by using (a) DMF, (b) DMA (Dimethylamine), (c) mixture of HNO_3 and DMF, and (d) liquid recovered from the former ionothermal treatment (150 ºC,12.0 h) as the solvent, respectively.

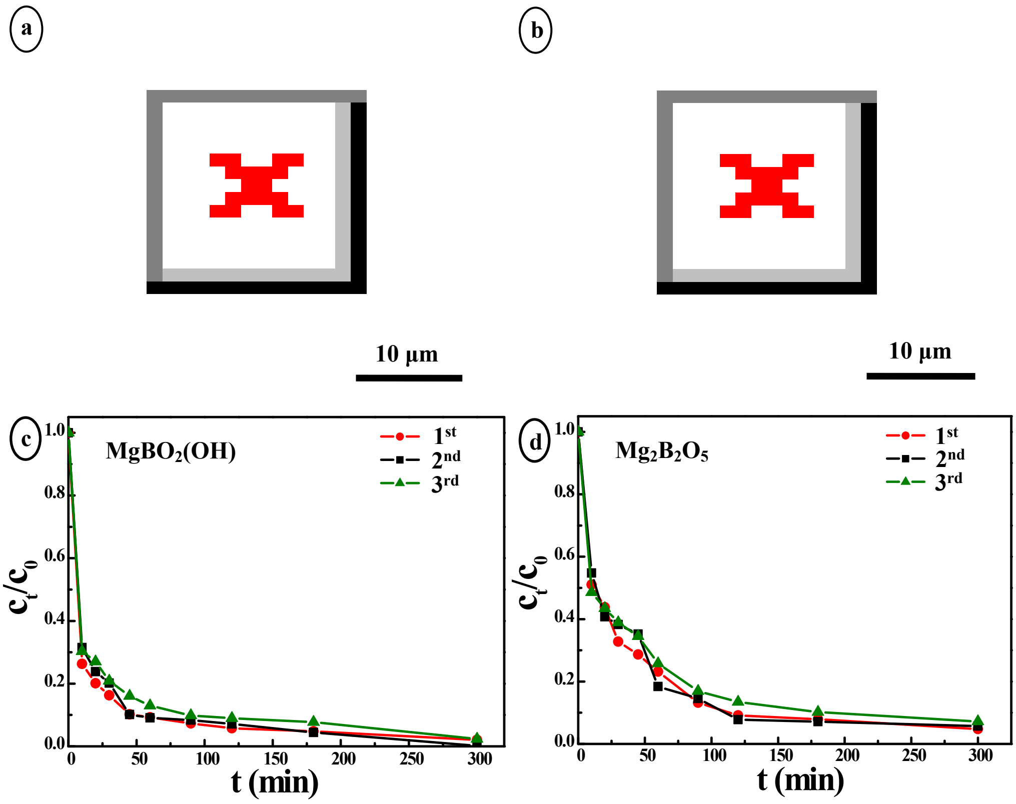

Fig. S6. SEM images of the regenerated $MgBO_2(OH)$ (a) and $Mg_2B_2O_5$ (b) superstructures by calcining the corresponding adsorbents containing previously adsorbed CR at 400 ºC for 2.0 h with a heating rate of 2 ºC min^{-1}, and the adsorption performances of the regenerated $MgBO_2(OH)$ (c) and $Mg_2B_2O_5$ (d) superstructures when used as the adsorbents for the second (–■–) and third (–▲–) time, with the first (–●–) time for comparison.

Table S1. Parameters of the isotherm models for the adsorption of CR onto the $MgBO_2(OH)$ and $Mg_2B_2O_5$ superstructures at room temperature with an initial concentration of 50 mg L^{-1}.

Samples	Langmuir isotherm model			Freundlich isotherm model		
	q_m (g mg^{-1})	b (L mg^{-1})	R^2	k_f	$1/n$	R^2
$MgBO_2(OH)$	228.3	0.64	0.9903	98.22	0.17	0.8890
$Mg_2B_2O_5$	139.3	0.98	0.9903	68.96	0.14	0.8766

Table S2. Parameters of the kinetic models for the adsorption of CR onto the $MgBO_2(OH)$ and $Mg_2B_2O_5$ superstructures at room temperature with an initial concentration of 50 mg L^{-1}.

Samples	$q_{e,exp}$	pseudo-first-order kinetic model			pseudo-second-order kinetic model		
	(g mg^{-1})	$q_{e,calc1}$ (g mg^{-1})	k_1 (min^{-1})	R^2	$q_{e,calc2}$ (g mg^{-1})	k_2 (mg g^{-1} min^{-1})	R^2
$MgBO_2(OH)$	97.94	26.57	0.0096	0.6192	99.01	0.0024	0.9995
$Mg_2B_2O_5$	96.59	57.59	0.0130	0.9244	97.09	0.0009	0.9967

Table S3. Parameters of the intra-particle diffusion model for the adsorption of CR onto the $MgBO_2(OH)$ and $Mg_2B_2O_5$ superstructures at room temperature with an initial concentration of 50 mg L^{-1}.

Samples	k_{dif1} (mg g^{-1} $h^{-1/2}$)	k_{dif2} (mg g^{-1} $h^{-1/2}$)	c_1 (mg g^{-1})	c_2 (mg g^{-1})
$MgBO_2(OH)$	34.78	5.53	59.54	85.76
$Mg_2B_2O_5$	45.96	6.89	30.04	78.64